

time-quantization and noise added to signal. This results in low-pass filtering of the averaged signal cycles. The low-pass filter characteristic is described by the distribution of the fiducial point jitter. The effect of low-pass filtering is reduced when robust weighted averaging is used (see Fig. 2). In this case, signal cycles only slightly similar to the averaged signal have small weights and their influence on the averaged signal is lower.

It can be noted that the running time of both the ε WAILP and ε WAILPADIP methods is significantly shorter (over 16 times) with respect to the ε WACFM method. However, it is still over 25 times greater with respect to traditional averaging.

Finally, it can be pointed out that our approach differs from other approaches aimed at reducing the effect of outliers. Usually a measure of similarity between signal cycles is used to identify outliers (see, e.g., [7] and [12]) at the stage of weights determination [see (4)], which may be called a global method. In the present method, it is also realized, however, that outliers are also reduced in the stage of the averaged signal \mathbf{v} determination. This approach may be called a local method. In other words, our method has two mechanisms of outliers reduction—a global one which reduces ectopic, QRS-like artifacts and a local one which reduces single-point outliers. The proposed algorithm does not exclude a whole signal cycle when only a short part of it is corrupted. The global method of outliers reduction may be used to identify abnormalities (nondominant signal cycles) in a biomedical signal—for example, in cardiac monitoring. It must also be stated that local methods of outliers reduction are known from literature [13], [14]. Median and alpha-trimmed means are good examples. However, these methods can be used in an equally weighted manner only. Thus, they cannot include directly a global mechanism of outliers reduction.

V. CONCLUSION

This paper proposes a new computationally effective algorithm to robust weighted averaging. This method eliminates one of the greatest disadvantages of traditional and weighted methods, that is, their sensitivity to the presence of outliers caused by, e.g., spike artifacts, included cycles with nondominant morphology, bursts of noise, and baseline shifts. Moreover, this approach has important advantages: 1) a reduced computational burden and 2) an automatic adjustment of the insensitivity parameter. The above features open the possibility of application of the robust weighted averaging in digital processing systems in which real-time or faster processing must be used.

ACKNOWLEDGMENT

The authors are grateful to the anonymous referees for their constructive comments that have helped to improve the paper. They would like to thank Dr. J. Jeżewski and his staff for granting permission to use FECG records.

REFERENCES

- [1] Z. Fan and T. Wang, "A weighted averaging method for evoked potential based on the minimum energy principle," in *Proc. Conf. IEEE EMBS*, vol. 13, 1991, pp. 411–412.
- [2] —, "Weighted averaging method for evoked potential: Determination of weighted coefficients," in *Proc. Conf. IEEE EMBS*, vol. 14, 1992, pp. 2473–2474.
- [3] C. E. Davila and M. S. Mobin, "Weighted averaging of evoked potentials," *IEEE Trans. Biomed. Eng.*, vol. 39, pp. 338–345, Apr. 1992.
- [4] E. Bataillou, E. Thierry, H. Rix, and O. Meste, "Weighted averaging using adaptive estimation of the weights," *Signal Processing*, vol. 44, pp. 51–66, 1995.
- [5] J. Łęski, "Application of time domain signal averaging and Kalman filtering for ECG noise reduction," Ph.D. dissertation, Silesian Univ. Technol., Gliwice, Poland, 1989.

- [6] —, "New concept of signal averaging in time domain," in *Proc. Conf. IEEE EMBS*, vol. 13, 1991, pp. 367–368.
- [7] J. Łęski and N. Henzel, "Biomedical signal averaging with highly-quantized weights," in *Proc. Conf. BMES/EMBS*, Atlanta, GA, 1999, p. 1013.
- [8] J. Łęski, "Robust weighted averaging," *IEEE Trans. Biomed. Eng.*, vol. 49, pp. 796–804, Aug. 2002.
- [9] A. Navia-Vázquez, F. Pérez-Cruz, A. Artés-Rodríguez, and A. R. Figueiras-Vidal, "Weighted least squares training of support vector classifiers leading to compact and adaptive schemes," *IEEE Trans. Neural Networks*, vol. 12, pp. 1047–1059, Sept. 2001.
- [10] J. M. Mendel, *Optimal Seismic Deconvolution. An Estimation-Based Approach*. New York: Academic, 1983.
- [11] P. Bergveld, A. J. Kölling, and J. H. J. Peuscher, "Real-time fetal ECG recordings," *IEEE Trans. Biomed. Eng.*, vol. BME-33, pp. 505–509, May 1986.
- [12] P. R. B. Barbosa, J. Barbosa-Filho, C. A. M. de Sa, E. C. Barbosa, and J. Nadal, "Reduction of electromyographic noise in the signal-averaged electrocardiogram by spectral decomposition," *IEEE Trans. Biomed. Eng.*, vol. 50, pp. 114–117, Jan. 2003.
- [13] D. Mämpel, A. K. Nandi, and K. Schellhorn, "Unified approach to trimmed mean estimation and its application to bispectrum estimation of EEG signals," *J. Franklin Inst.*, vol. 333, no. 3, pp. 369–383, 1996.
- [14] V. X. Afonso, W. J. Tompkins, T. Q. Nguyen, K. Michler, and S. Luo, "Comparing stress ECG enhancement algorithms," *IEEE Eng. Med. Biol. Mag.*, vol. 15, pp. 37–44, May/June 1996.

Assessing Blood Flow Control Through a Bootstrap Method

David M. Simpson*, Ronney B. Panerai, Eloane G. Ramos,
José Maria A. Lopes, Monica N. Villar Marinatto, Jurandir Nadal,
and David H. Evans

Abstract—In order to assess blood flow control, the relationship between blood pressure and blood flow can be modeled by linear filters. We present a bootstrap method, which allows the statistical analysis of an index of blood flow control that is obtained from constrained system identification using an established set of pre-defined filters.

Index Terms—Bootstrap method, cerebral blood flow control, system identification.

I. INTRODUCTION

The mechanisms of blood flow autoregulation maintain an approximately constant blood supply to the brain, even if blood pressure varies over a considerable range [1]. Impairment of this control system can lead to cerebral hypo- or hyper-perfusion and may result in temporary or permanent brain damage or even death. In spite of the great clinical interest, testing the integrity of autoregulation remains a major

Manuscript received February 14, 2003; revised October 19, 2003. This work was supported by the Wellcome Trust (Project Number 064701/Z/01/Z) and the Brazilian Research Council (CNPq). *Asterisk indicates corresponding author.*

D. M. Simpson* is with the Institute of Sound and Vibration Research, University of Southampton, Southampton SO17 1BJ, U.K. (e-mail: ds@isvr.soton.ac.uk).

R. B. Panerai and D. H. Evans are with the Department of Cardiovascular Science, Faculty of Medicine, University of Leicester, Leicester LE1 7RH, U.K., and also with the Department of Medical Physics, Leicester Royal Infirmary, Leicester, LE1 5WW, UK.

E. G. Ramos and J. Nadal are with the Biomedical Engineering Program Federal University of Rio de Janeiro, CP 68510, 21945-970 Rio de Janeiro.

J. M. A. Lopes and M. N. V. Marinatto are with the Neonatal Intensive Care Unit Instituto Fernandes Figueira Av. Rui Barbosa 716 22250-020 Rio de Janeiro.

Digital Object Identifier 10.1109/TBME.2004.827947

technical challenge [2], and no gold standard for its assessment has been established so far. Autoregulation is evident from the relationship between spontaneous changes in arterial blood pressure (ABP) and cerebral blood flow (or, more commonly, cerebral blood flow velocity (CBFV) as measured by transcranial Doppler ultrasound), and this can be exploited in testing autoregulation even in haemodynamically vulnerable patients, including neonates.

Constrained system identification was employed by Panerai *et al.* [3] on such spontaneously varying data by grading autoregulation based on a predefined set of 10 linear filters [4]. The current work extends their approach, for which we present a bootstrap method to assess the statistics of their autoregulation index (ARI). This gives an indication of the robustness of an ARI estimate and allows the statistical significance of any changes in a patient's ARI to be tested. To the best of our knowledge, bootstrap methods have not previously been used in this type of problem.

II. METHODS

ABP and CBFV signals were simultaneously collected from 40 newborn babies (term and preterm) in the neonatal intensive care unit of Instituto Fernandes Figueira (FIOCRUZ, Rio de Janeiro, Brazil). The local ethics committee approved the study, and parental consent was obtained. The cases selected reflect the type of patients in whom autoregulation is of clinical interest. ABP was measured in the umbilical artery and CBFV in the middle cerebral artery. Following procedures in previous work [3], the mean CBFV and ABP for each heart-beat were found, and the resultant signal interpolated to a sampling rate of 5 Hz. The signals were then normalized to give the percentage variation in the data. A total of 127 signals were analyzed, and only recordings greater than 150 s in duration were included (duration 260 ± 103 s; mean \pm standard deviation). The autoregulation index for each patient recording was then obtained following the method used previously [3]: to the ABP signal a set of 10 predefined linear filters [4] was applied, with the output of each giving an estimate of CBFV. The filters represent the range from absent autoregulation (ARI = 0) to excellent autoregulation (ARI = 9). The output that gives the best match between measured and estimated CBFV is then selected, providing the ARI for the recorded data.

Significance tests of changes in any patient's ARI over time, and the estimation error in any individual ARI estimate cannot readily be evaluated using conventional statistical methods. The bootstrap approach [5]; [6] provides a convenient and very flexible alternative, which can be adapted to the constrained system identification employed here. The bootstrap method is based on randomly resampling (with replacement) the original data, thus generating additional (surrogate) data [5]; [6]. For signals with nonzero correlation between samples (i.e., nonwhite data), the moving block (or block-wise) bootstrap [7] should be employed, where randomly selected blocks of samples make up the "bootstrapped signals." This can be applied to the ARI estimates in the following way: first, the number of bootstrap blocks (M) is chosen and the number of samples in each block found as $L = N/M$ (rounded to the nearest integer), where N is the length of the signal. For the first of the bootstrap signals, the start of each block ($i_m, m = 1 \dots M$) is then found by generating M random integer numbers uniformly distributed in the range $0 \dots N - L$. The bootstrap signals of measured CBFV $v(n)$ (denoted by $v^*(n)$); * denotes a bootstrap signal or parameter estimate) as well as the estimated CBFV $v_{\text{ARI}}(n)$ ($v_{\text{ARI}}^*(n)$), the filter outputs for ARI = 0...9) are then obtained by concatenating the samples $[i_1 \dots i_1 + L - 1, i_2 \dots i_2 + L - 1, \dots, i_M \dots i_M + L - 1]$ from the corresponding signals. From these synthetic signals, a bootstrap estimate of ARI is obtained (ARI*) by finding the $v_{\text{ARI}}^*(n)$ that best matches $v^*(n)$ (i.e., following the same procedure used for the original patient data). Note that since all bootstrapped signals have the discontinuities between blocks at the same instants in time, this does not affect the goodness-of-fit between measured and estimated CBFV. The next

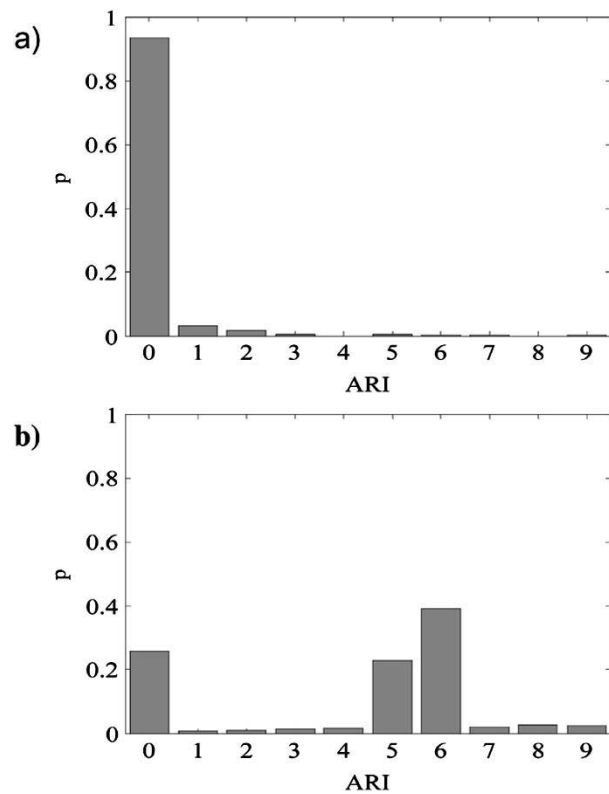


Fig. 1. Examples of the ARI histograms obtained from bootstrap resampling in two different patient records. p is the relative frequency of the bootstrap ARI estimates. The ARI estimated for the original patient records were (a) ARI = 0 and (b) ARI = 5.

bootstrap estimate (ARI*) is then obtained by selecting a new set of random start values (i_m). This process is repeated to obtain $K = 499$ bootstrap estimates, resulting in a histogram of ARI estimates (Fig. 1 gives two examples).

In order to test the null hypothesis that the ARI in two different patient recordings is identical ($H_0 : \Delta \text{ARI} = |\text{ARI}_2 - \text{ARI}_1| = 0$), an approach similar to that used in two-sample tests of the difference in mean value is followed. Thus, the difference in the ARI estimates from the patient recordings is compared with the dispersion of the histograms obtained from the bootstrap method.

III. RESULTS

The histograms of bootstrapped ARI estimates indicate the dispersion of ARI estimates from a single recording (Fig. 1). The results were found to vary widely across 127 patient recordings: in some cases, the ARI estimates appear very robust [a single sharp peak in the histogram, Fig. 1(a)], but in others there is considerable spread, and bimodal distributions are common [Fig. 1(b)]; some histograms even show modes at both ARI = 0 and ARI = 9. The standard deviation of the bootstrapped ARI estimates was correlated with both the coefficient of variation of the ABP signal ($r = -0.35, p < 10^{-4}$), and the mean-square error of the model fit ($r = 0.63, p < 10^{-15}$). Bootstrap tests for significant differences in ARI estimates between consecutive recordings in each subject (87 tests in the 40 patients), detected no statistically significant changes ($p > 0.05$), though ARIs fluctuated widely. A paired t-test showed that as a group, the patients' ARI increased over time ($p = 0.03$).

The bootstrap method was also evaluated using simulated signals. To this end, random signals were generated with a spectrum similar to that of a patient's ABP. CBFV was then obtained by applying each of the ten filters in turn to the ABP and adding noise whose spectrum matches that

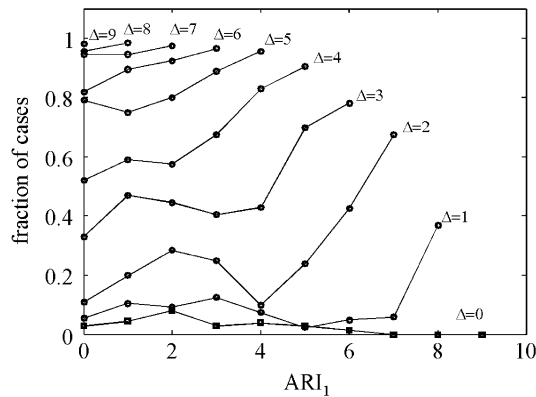


Fig. 2. Simulation results, presenting the fraction of cases in which differences between pairs of estimated ARIs were found to be significant, at the $\alpha = 5\%$ level. The horizontal axis gives the ARI of the first signal (ARI_1 , as used in generating the simulated data). That of the second signal $ARI_2 = ARI_1 + \Delta$, where Δ is the difference in the ARIs. ARI_1 and ARI_2 range from 0 to 9, and 200 pairs of signals were simulated.

of the noise estimated from the patient recordings. This was repeated 200 times. The ARI was then estimated for each of the simulated signals, and the bootstrap method applied in order to test the significance of any difference in ARI estimates. The results (Fig. 2) show that, when the “true” ARIs (i.e., the ones corresponding to the filter actually used in generating the simulated signals) are identical ($\Delta = 0$), the expected $\alpha = 5\%$ false positive rate is approximated. However, fewer false positives are detected for $ARI > 5$, since here the estimator generally finds the correct ARI such that there is no difference in ARI estimates. As the difference between the ARIs increases ($\Delta > 0$), the fraction of cases in which significant differences are found also increases—as expected.

IV. DISCUSSION AND CONCLUSION

The bootstrap method presented provides a relatively simple means for statistical analysis of the ARI. The method is intuitively meaningful, and simulation studies provided further supporting evidence for its use. The results with the patient data indicate that the ARI estimate is not always robust. This had been suspected from the wide variations over time in ARI estimates from the patients, but now the bootstrap method provides confirmation that even within a given recording, ARI estimates can be inconsistent. Short-term variations in autoregulatory activity, nonlinear system characteristics [2], as well as the influence of other physiological variables (e.g., CO_2 and O_2 levels and intracranial pressure variations [1]) on CBFV probably all contribute to the variability of ARI estimates. The proposed bootstrap method now permits quantitative measures (e.g., standard deviation) of the estimation error in the ARIs to be determined, for each recording. This can provide an objective criterion for selecting signals that lead to more robust ARI estimates (e.g., higher variability of ABP and better model fit both were seen to lead to reduced standard deviation), as well as providing a solid basis for the future development of improved filter sets (including nonlinear ones).

While we have applied the proposed bootstrap solution in the analysis of autoregulatory activity, we hope that the method will prove useful in a wider range of problems in constrained system identification for physiological applications.

ACKNOWLEDGMENT

The authors are grateful to Dr. L. Fan for the development of the Doppler system used in this work.

REFERENCES

- [1] O. B. Paulson, S. Strandgaard, and L. Edvinson, “Cerebral autoregulation,” *Cerebrovasc. Brain Metab. Rev.*, vol. 2, pp. 161–192, 1990.
- [2] R. B. Panerai, “Assessment of cerebral pressure autoregulation in humans—A review of measurement methods,” *Phys. Meas.*, vol. 19, pp. 305–338, 1998.
- [3] R. B. Panerai, S. L. Dawson, P. J. Eames, and J. F. Potter, “Cerebral blood flow velocity response to induced and spontaneous sudden changes in arterial blood pressure,” *Amer. J. Physiol.*, vol. 280, pp. H2162–H2174, 2001.
- [4] F. P. Tiecks, A. M. Lam, R. Aaslid, and D. W. Newell, “Comparison of static and dynamic cerebral autoregulation measurements,” *Stroke*, vol. 26, pp. 1014–1019, 1995.
- [5] D. N. Politis, “Computer intensive methods in statistical analysis,” in *IEEE Signal Processing Mag.*, vol. 15, Jan 1998, pp. 39–55.
- [6] A. M. Zoubir and B. Boashash, “The bootstrap and its application in signal processing,” in *IEEE Signal Processing Mag.*, vol. 15, Jan. 1998, pp. 56–76.
- [7] H. Li and G. S. Maddala, “Bootstrapping time series models,” *Econometric Rev.*, vol. 15, no. 2, pp. 115–158, 1996.

A Computer-Aided Diagnosis for Distinguishing Tourette’s Syndrome From Chronic Tic Disorder in Children by a Fuzzy System With a Two-Step Minimization Approach

Tang-Kai Yin* and Nan-Tsing Chiu

Abstract—Tourette’s syndrome, no longer considered as a rare and unusual disease, is the most severe tic disorder in children. Early differential diagnosis between Tourette’s syndrome and chronic tic disorder is difficult but important because proper and early medical therapy can improve the child’s condition. Brain single-photon emission computed tomography (SPECT) perfusion imaging with technetium-99m hexamethylpropylene amine oxime is a method to distinguish these two diseases. In this paper, a fuzzy system called characteristic-point-based fuzzy inference system (CPFIS) is proposed to help radiologists perform computer-aided diagnosis (CAD). The CPFIS consists of SPECT-volume processing, input-variables selection, characteristic-points (CPs) derivation, and parameter tuning of the fuzzy system. Experimental results showed that the major fuzzy rules from the obtained CPs match the major patterns of Tourette’s syndrome and chronic tic disorder in perfusion imaging. If any case that was diagnosed as chronic tic by the radiologist but as Tourette’s syndrome by the CPFIS was taken as Tourette’s syndrome, then the accuracy of the radiologist was increased from 87.5% (21 of 24) without the CPFIS to 91.7% (22 of 24) with the CPFIS. All 17 cases of Tourette’s syndrome, which is more severe than chronic tic disorder, were correctly classified. Although the construction and application process of the proposed method is complete, more samples should be used and tested in order to design a universally effective CAD without small sample-size concerns in this research.

Index Terms—AI approaches, biosignal interpretation and diagnostic systems, fuzzy systems, signal and image processing.

I. INTRODUCTION

Tic disorders can be motor tics, vocal tics, or both. They are involuntary, sudden, and repetitive movements or vocalizations. It is esti-

Manuscript received September 9, 2002; revised October 7, 2003. This work was supported in part by the National Science Council under Grant NSC-90-2213-E-041-005. Asterisk indicates corresponding author.

*T.-K. Yin is with the Department of Management Information Science, Chia-Nan University of Pharmacy and Science, Tainan, Taiwan, R.O.C. (e-mail: qtkyin@mail.chna.edu.tw).

N.-T. Chiu is with the Department of Nuclear Medicine, College of Medicine, National Cheng Kung University, Tainan, Taiwan, R.O.C.

Digital Object Identifier 10.1109/TBME.2004.827954